Photomedicine and Laser Surgery
Volume 26, Number 2, 2008

Pp. 83–90
DOI: 10.1089/pho.2007.2128

Diagnosis of Ovarian Cancer by Raman Spectroscopy: A Pilot Study

K. MAHEEDHAR, M.Sc.,[1] RANI A. BHAT, M.D.,[2] R. MALINI, M.Sc.,[3]
N.B. PRATHIMA, M.Sc.,[3] PATIL KEERTHI, B.Sc.,[3] PRALHAD KUSHTAGI, M.D.,[2]
and C. MURALI KRISHNA, Ph.D.[3]

ABSTRACT

Objective: **To assess the efficacy of conventional Raman spectroscopy in combination with discriminating parameters, Mahalanobis distance, spectral residuals, and "limit test" methodology in differentiation of normal and malignant ovarian tissues.** ***Background Data:*** **Ovarian cancer is the second most common cancer among women and the leading cause of death among gynecologic malignancies. Initial laparotomy and subsequent frozen section analysis can influence the surgical management of ovarian cancers. Although frozen section pathology is sensitive and specific enough, interpretation is often subjective, time consuming, and requires highly skilled personnel. Raman spectroscopy is sensitive to biochemical variations in the samples, rapid, more objective, and amenable to multivariate statistical tools. It can therefore be an ideal tool for discrimination between normal and malignant ovarian tissues.** ***Methods:*** **72 Spectra from eight normal and seven malignant ovarian tissues were recorded by conventional near-infrared (NIR) Raman spectroscopy (excitation wavelength of 785 nm). Spectral data were analyzed by principal components analysis (PCA) and other discriminating parameters such as Mahalanobis distance, spectral residuals, and a multiparametric limit test approach.** ***Results:*** **A mean malignant spectrum exhibits a broader amide I band, a stronger amide III band, a minor blue shift in the δCH_2 band, and a hump around 1480 cm^{-1} compared to a normal spectrum. The normal spectra show relatively stronger peaks around the 855 and 940 cm^{-1} region. Scores of factor 1 as well as Mahalanobis distance and spectral residuals gave good classification among the tissue types. The limit test approach provided unambiguous and objective discrimination.** ***Conclusion:*** **The findings of this study demonstrate the efficacy of conventional Raman spectroscopy and our statistical methodologies in discrimination of normal from malignant ovarian tissues. Prospectively, by evaluating the models and developing suitable fiberoptic probes, this technique could be useful in diagnosis during initial laparotomy.**

INTRODUCTION

OVARIAN CANCER is the second most common gynecological malignancy. It accounts for 4% of all cancers among women, and is the leading cause of death from gynecologic malignancy. Early-stage ovarian cancer is generally asymptomatic. Approximately 75% of women are diagnosed only at an advanced stage. Survival is highly dependent on stage of disease: 5-year survival is around 80%–90% for early cancers, which decreases to 25% for advanced stages of disease.[1,2] It has been shown that new prevention strategies such as early diagnosis hold significant promise to reduce mortality and in turn improve prognosis.[3] The greatest opportunity to influence the natural history of ovarian cancer occurs at the initial laparotomy and subsequent frozen section pathology, which allows intraoperative evaluation to distinguish benign from malignant tumors in order to determine the extent of surgery necessary. Though it has certain disadvantages, such as loss of structural details, it is sufficiently sensitive and specific for clinical use. Generally, the false-negative rate is low and the false-positive rate is neg-

[1]Division of Laser Spectroscopy, Manipal Life Science Center/Department of Radiotherapy and Oncology, Shirdi Sai Baba Cancer Hospital, [2]Department of Obstetrics and Gynecology, Kasturba Medical College, Manipal University, [3]Division of Laser Spectroscopy, Manipal Life Science Center, Manipal University, Manipal, Karnataka, India.

ligible.[4,5] However, frozen section analysis is time consuming, requires highly skilled personnel, and interpretation is often subjective. Hence, there is a need for an alternate intraoperative diagnostic tool which is rapid, inexpensive, equally sensitive as frozen section pathology, and most importantly, can be adapted to *in vivo/in situ* conditions.

Among the leading methods to perform such assays, optically-based methods hold great promise.[6–9] These methods are rapid and objective, as data are amenable to multivariate statistical analytical tools. The emerging popularity of Raman spectroscopy can be attributed to the unique advantages it offers, which include use of less harmful near-infrared (NIR) radiation for excitation, adaptability for *in situ/in vivo* measurements, minimal or no requirement for sample preparation, and easy extraction of information content. As is evident from the literature, very few studies on ovarian cancer diagnosis by spectroscopy methods, autofluorescence, reflectance spectroscopy, Fourier transform infrared (FTIR), and Raman spectroscopy have been reported.[10–13] Efficacy of the proteomics pattern of serum samples as a screening tool in ovarian cancers has also been reported.[14] Discrimination of normal and pathological formalin-fixed ovarian tissues by FTIR and Raman microspectroscopy has also been reported.[15,16]

In the present study, conventional Raman spectroscopic study of ovarian cancers was carried out in order to explore an alternative to frozen section evaluation of tissues at surgery. This approach has the advantage of providing representative spectral features from *ex-vivo* samples, which can be extrapolated or simulated to *in situ/in vivo* conditions to a large extent. As mentioned previously, one of the major advantages of spectroscopy is objective discrimination. This is feasible because of the amenability of spectral data to multivariate statistical tools, and several such statistical methods are now available to spectroscopists for data analysis and mining. Therefore, it is also necessary to explore different discriminate algorithms in order to develop robust, rapid, and simpler discriminating methods. In our earlier studies, we have demonstrated the potential of Mahalanobis distance, spectral residuals, and limit test approach in discriminating normal and malignant conditions in oral, breast, cervical, stomach, and colon tissues.[17–21] In the present study, we have extended the above data analysis approaches for discrimination of normal and malignant ovarian tissues. The results obtained in this study are discussed in this paper.

MATERIALS AND METHODS

Fresh tissue samples (from biopsy or surgical resection) were obtained in saline from the Department of Obstetrics and Gynecology, Manipal University, Manipal. In each case, a mirror image of the tissue sample was sent for histopathological certification. Spectra were recorded at several sites. A total of 72 certified spectra, 38 spectra of eight normal tissues and 34 spectra of seven malignant tissues, were analyzed in this study.

Laser Raman spectroscopy

Raman spectra were recorded with a set-up we assembled. This set-up consists of a diode laser (SDL-8530, 785 nm, 100 mW; Vin Karoba Instruments, Norcross, GA) for excitation and Raman signals were detected by an HR 320 spectrograph (600 g/mm blazed at 900 nm; Spex Triax, Jobin Yvon-Spex, Edison, NJ) coupled to a Spectrum One liquid-nitrogen cooled CCD (Jobin Yvon-Spex). A holographic filter (HLBF-785.0; Kaiser Optics, Ann Arbor, MI) was used to filter out unwanted lines from the excitation source. A notch filter (HSPF-5812; Kaiser Optics) was used to reject the Rayleigh scattering from the Raman signals. At each spectral point, signals were collected for 30 sec and averaged over 20 accumulations. The samples were kept moist with saline during spectral acquisition. The recorded spectra were calibrated with a cubic fit to known frequencies of acetaminophen.

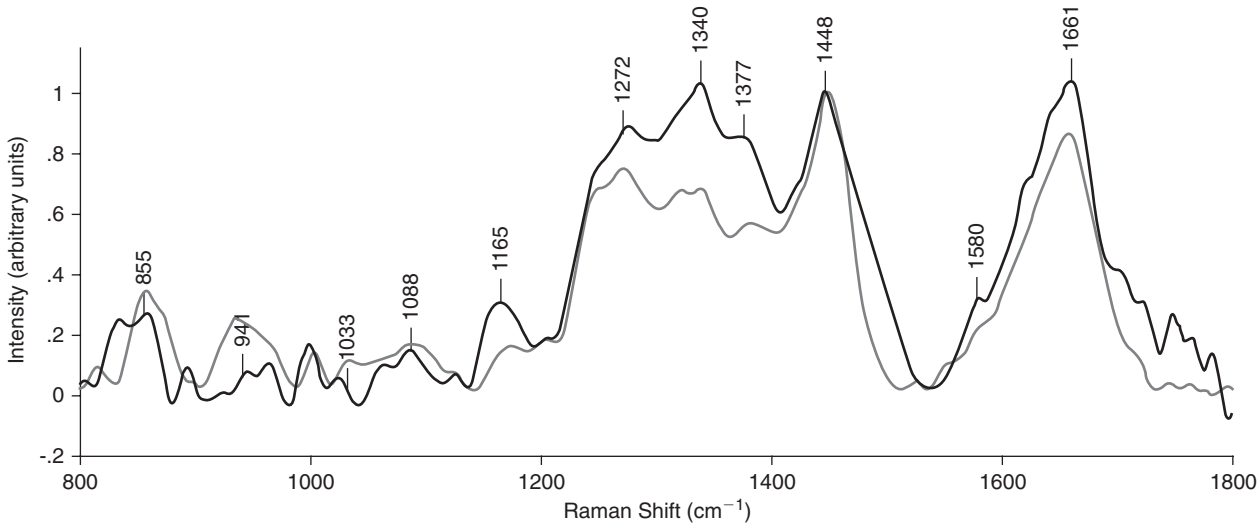

FIG. 1. Mean spectra of normal (grey) and malignant (black) ovarian tissues

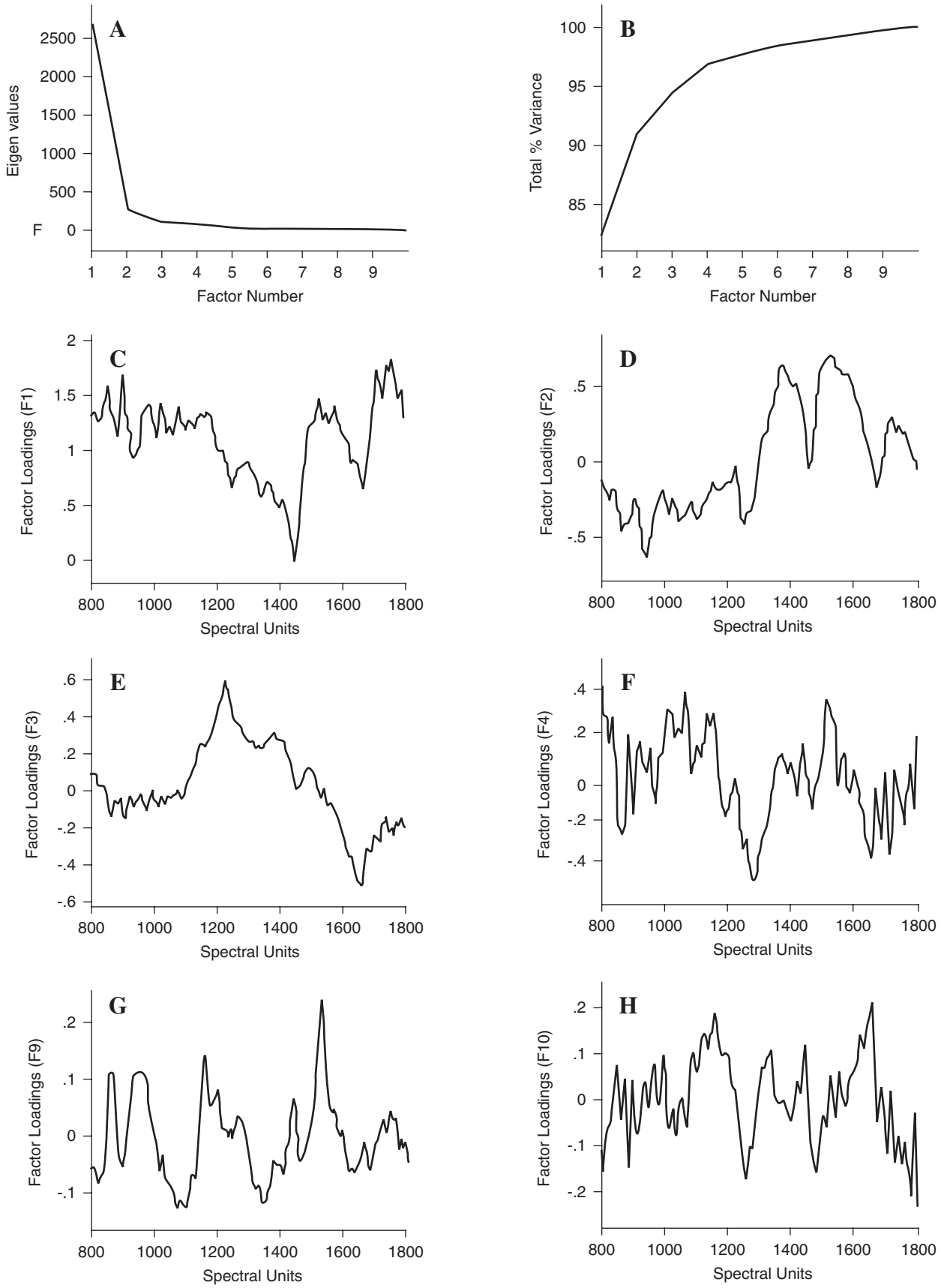

FIG. 2. PCA of ovarian tissues: factor profiles. (**A**) Eigenvalues. (**B**) Total percent of variance. (**C**) Loadings of factor 1. (**D**) Loadings of factor 2. (**E**) Loadings of factor 3. (**F**) Loadings of factor 4. (**G**) Loadings of factor 9. (**H**) Loadings of factor 10.

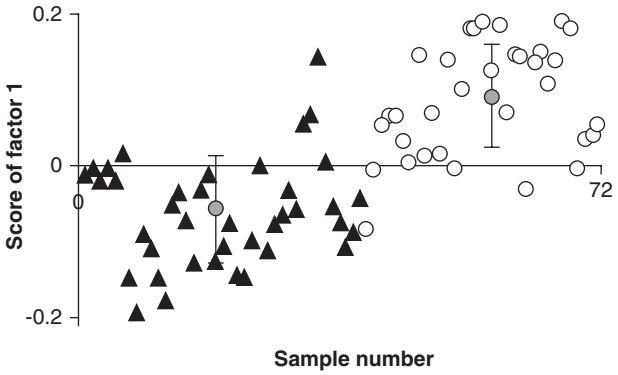

FIG. 3. PCA of Raman spectra of ovarian tissues: Plot of score of factor 1 vs. sample number (▲, normal; ○, malignant).

Data analysis

Baseline correction, smoothening, calibration, and normalization over δCH_2 were carried out using Grams 32 (Galactic Industries Corporation, Salem, NH). Principal components analysis (PCA) was carried in the 800–1800 cm^{-1} spectral range, and also other selected regions in this range using Grams PLS Plus/IQ (Galactic Industries Corporation). Trial runs of PCA were carried out employing 15, 10, and 6 factors. From the results of our trial runs, we determined that a spectral range of 800–1800 cm^{-1} with ten factors gave the best results. Total percentage of variance, eigenvalues, and factor profiles were employed for determining the number of significant factors for PCA. Further data analysis was carried out under these conditions. Two approaches were considered to achieve objective discrimination.

In the first approach, spectra of normal and malignant tissues were pooled and analyzed by PCA and scores of factors were used for discrimination of tissue types. In the second approach, standard calibration sets of randomly selected spectra from the pathologically certified groups were developed for normal and malignant tissues. All samples (including those in the calibration set, by rotating them out one at a time) were then matched against the calibration sets to compute Mahalanobis distance and spectral residuals. This approach was further extended to compute match/mismatch classification using a limit test approach.

RESULTS AND DISCUSSION

Typical mean Raman spectra of normal (grey line) and malignant (black line) ovarian tissues are shown in Fig. 1. The mean malignant spectrum exhibits a broader amide I band, stronger amide III band, a minor blue shift in the δCH_2 band, and a hump around 1480 cm^{-1} and other strong peaks around 834, 900, 1000, and 1165 cm^{-1} compared to the normal tissue spectrum. The normal spectra had relatively stronger peaks around 855 and 940 cm^{-1}. These spectral features of the mean malignant tissue spectra indicate the presence of additional biomolecules such as proteins (amide I, amide III, 845, 1000, 1165, and 1580 cm^{-1}), lipids (blue shift in δCH_2), and DNA (1340 cm^{-1} and a hump at 1480 cm^{-1}). Variations in the secondary structures of proteins is also suggested by spectral profiles in the 900–950 cm^{-1} region.[22,23] However, the spectra of ovarian tissues are relatively weaker than those of the other types of tissues, such as oral, cervical, and breast tissue, that we recorded using the same set-up.

As mentioned earlier, spectroscopists now have several options for data analysis, such as artificial neural network (ANN), K-means nearest neighbor (KNN), hierarchical cluster analysis (HCA), and principal components analysis (PCA). In the present work, PCA was employed to discriminate normal from malignant tissue types. Analysis was carried out using two different approaches. PCA is a well known method of data description and compression that can describe a large amount of spectral data by means of a small number of independent variables called eigenvectors, factors, or principal components, and the scaling constants used to reconstruct the spectra are known as scores. Scores of factors can be used as parameters for objective discrimination. Analysis was carried out using two different approaches. In the first approach unsupervised classification of 72 spectra combined from normal and malignant ovarian tissues were employed in the study. Profiles of the factor loadings of the first four factors contribute to 97% of the total variance, and the last two factors (factors 9 and 10) account for noise, as shown in Fig. 2. Fig. 3 shows the clustering of normal and malignant spectra based on the score of factor 1. The scores of factor 1 for normal spectra are generally negative, with a mean of -0.05 ± 0.068, and the malignant spectra show positive values, with a mean of 0.09 ± 0.0684. A minor overlap is observed between clusters even up to mean $\pm$ 1 standard deviation, which indicates a sensitivity and specificity of 75%.[24] We have also computed sensitivity and specificity based on true positive and true negative formulas, and their values are 87.5% and 83.8%, respectively, as shown in Table 1. Unsupervised classification based on scores of factor is a widely used approach to obtain discrimination between tissue types. However, this is a somewhat cumbersome and tedious procedure for routine diagnosis from the clinical point of view, as diagnosis of each case requires repetition of the entire analysis.

TABLE 1. SPECIFICITY AND SENSITIVITY OF DISCRIMINATING ALGORITHMS

Sample	*Discriminating algorithms*	*Sensitivity*	*Specificity*
PCA: Scores of factor			
1	Scores of factor 1 vs. sample number	87.5%	83.8%
Discriminant analysis: Mahalanobis distance vs. spectral residuals			
2	Verification: Malignant standard set	100%	100%
3	Evaluation: Malignant standard set	100%	100%
Limit test approach			
4	Multiparametric limit test approach using malignant standard set	100%	100%

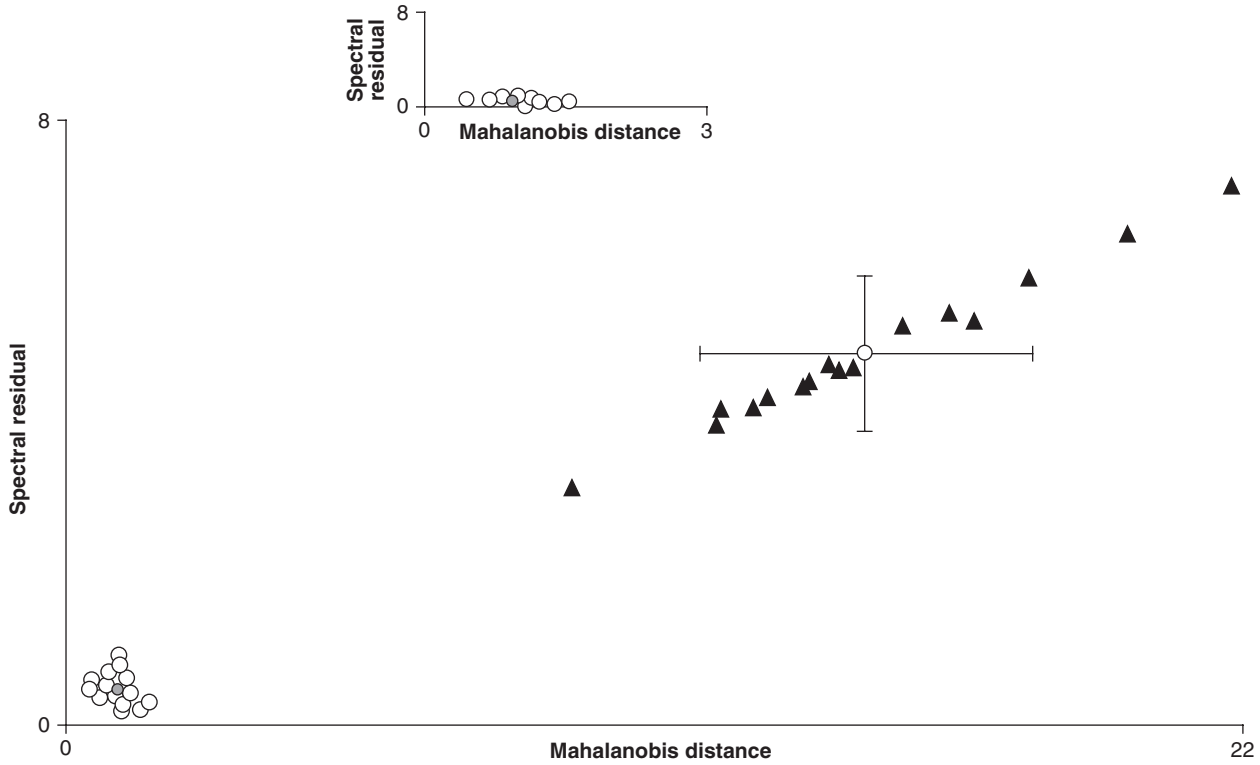

FIG. 4. PCA of Raman spectra of ovarian tissues: Verification of spectra used in the training set compared against a malignant training set (Mahalanobis distance vs. spectral residuals) (▲, normal; ○, malignant).

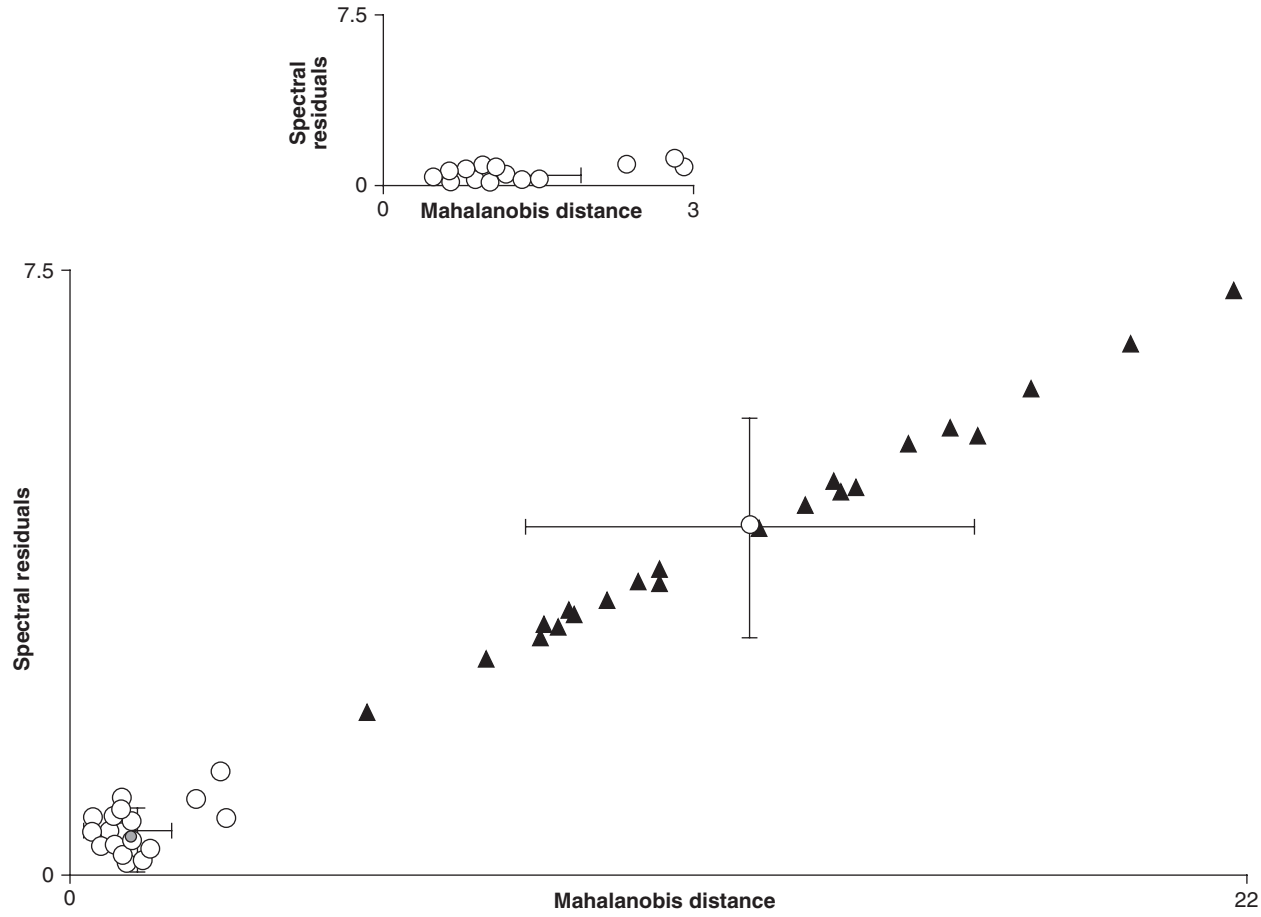

FIG. 5. PCA of Raman spectra of ovarian tissues: Evaluation by spectra not used in training sets against a malignant training set (plot of Mahalanobis distance vs. spectral residual) (▲, normal; ○, malignant).

In view of these considerations, we have also considered another approach based on multiple discriminating parameters to give a better and more objective diagnosis. For this method, as for any other analytical technique, standard sets are developed using a set of spectra from certified samples and then subjected to PCA to derive parameters that will be highly characteristic for any sample of that type. These sets can be used to decide whether a given spectrum belongs to that set, and if so, with what statistical probability. Thus, besides score of factors, PCA provides several other discriminating parameters for classification, once standard sets are developed. Mahalanobis distance (a measure of proximity of two spectra) and spectral residuals (squared error sum of difference between recorded and simulated spectrum) are two such parameters. Theory, method of calculation, and the advantages of these parameters for discrimination purposes are discussed elsewhere.[17–20] When compared with training sets, if Mahalanobis distance of a test spectrum has values more than 3, it will have a probability of 0.5% or less of being classified as the same class against which the spectrum is being compared. The Mahalanobis distance is normally expressed in units of standard deviation. In the present analysis it is given by:

$$D^2 = (S_{test})\ M^{-1}\ (S_{test})'$$

where S_{test} is the vector of the scores and sum of squared spectral residuals for a given test sample, and M is given by $M = S'S/(n - 1)$, where S contains the corresponding parameters for the calibration set (n standards).[24–25] The advantage of D^2 is discussed in our earlier papers.[17–20]

In the present analysis, we randomly selected 18 normal and 16 malignant spectra based on a score of factor 1, and histopathological certification was used in developing the training sets. The consistency of the training sets was verified by rotating spectra from training sets and comparing them against both training sets. Spectra corresponding to the same class of training sets should yield lower Mahalanobis distance and spectral residual values, and vice versa. As an example, results obtained against a malignant training set are shown in Fig. 4. From the figure, we can see that quite good discrimination between

Table 2. Match/Mismatch Table for All Samples Compared Against the Malignant Calibration Set

Sample	*Match*	*Limit Tests*	*Sample*	*Match*	*Limit tests*
1	YES	PASS (PPP#)	37	NO	FAIL (PPF#)
2	YES	PASS (PPP#)	38	NO	FAIL (PPF#)
3	YES	PASS (PPP#)	39	NO	FAIL (PPF#)
4	YES	PASS (PPP#)	40	NO	FAIL (P?F#)
5	YES	PASS (PPP#)	41	NO	FAIL (PPF#)
6	POSSIBLE	PASS (PP?#)	42	NO	FAIL (FPF#)
7	YES	PASS (PPP#)	43	NO	FAIL (FPF#)
8	YES	PASS (PPP#)	44	NO	FAIL (F?F#)
9	YES	PASS (PPP#)	45	NO	FAIL (PPF#)
10	YES	PASS (PPP#)	46	NO	FAIL (P?F#)
11	YES	PASS (PPP#)	47	NO	FAIL (F?F#)
12	POSSIBLE	PASS (PP?#)	48	NO	FAIL (PFF#)
13	POSSIBLE	PASS (PP?#)	49	NO	FAIL (F?F#)
14	POSSIBLE	PASS (PP?#)	50	NO	FAIL (F?F#)
15	YES	PASS (PP?#)	51	NO	FAIL (F?F#)
16	YES	PASS (PPP#)	52	NO	FAIL (P?F#)
17	POSSIBLE	PASS (PP?#)	53	NO	FAIL (F?F#)
18	YES	PASS (PP?#)	54	NO	FAIL (FFF#)
19	POSSIBLE	FAIL (FP?#)	55	NO	FAIL (F?F#)
20	YES	PASS (PPP#)	56	NO	FAIL (F?F#)
21	YES	PASS (PPP#)	57	NO	FAIL (FFF#)
22	POSSIBLE	PASS (PP?#)	58	NO	FAIL (FFF#)
23	YES	PASS (PPP#)	59	NO	FAIL (F?F#)
24	YES	PASS (PPP#)	60	NO	FAIL (F?F#)
25	POSSIBLE	PASS (PP?#)	61	NO	FAIL (FFF#)
26	YES	PASS (PP?#)	62	NO	FAIL (FFF#)
27	POSSIBLE	PASS (PP?#)	63	NO	FAIL (F?F#)
28	POSSIBLE	PASS (PP?#)	64	NO	FAIL (FFF#)
29	YES	PASS (PPP#)	65	NO	FAIL (F?F#)
30	YES	PASS (PPP#)	66	NO	FAIL (F?F#)
31	YES	PASS (PP?#)	67	NO	FAIL (F?F#)
32	YES	PASS (PPP#)	68	NO	FAIL (F?F#)
33	YES	PASS (PPP#)	69	NO	FAIL (FFF#)
34	POSSIBLE	PASS (PP?#)	70	NO	FAIL (F?F#)
35	NO	FAIL (FPF#)	71	NO	FAIL (FFF#)
36	NO	FAIL (PPF#)	72	NO	FAIL (F?F#)

the tissues was achieved. The mean Mahalanobis distance values of malignant and normal spectra are 0.92 ± 0.29 and 14.9 ± 3.07, respectively. The mean spectral residual values for malignant and normal spectra are 0.47 ± 0.40 and 4.97 ± 1.0, respectively. Based on the true-positive and true-negative formulas, the computed sensitivity and specificity values for this approach are 100% (Table 1).

These training sets are further evaluated by spectra that are not involved in training sets. Once again test spectra are compared against both the training sets. Fig. 5 shows typical results obtained against a malignant training set and good discrimination is achieved. The mean Mahalanobis distance for malignant and normal spectra are 1.18 ± 0.70 and 12.17 ± 4.18, respectively. The mean spectral residual values for malignant and normal spectra are 0.53 ± 0.26 and 4.26 ± 1.24, respectively. Once again 100% sensitivity and specificity, based on true-positive and true-negative methodology, was observed as shown in Table 1. Thus in both the approaches a clear discrimination between normal and malignant spectra was observed. However, computation of sensitivity and specificity based on smaller data sets could be erroneous. The approach of computing Mahalanobis distance and spectral residuals is further extended to the multi-parametric "limit test" approach.[17–20] It is a typical match/mismatch approach against a training set. In this analysis a given spectrum is compared with fixed values of inclusion/exclusion criteria for Mahalanobis distance, spectral residuals, and score of factors. If the values of a given spectrum are within the set limits, then the spectrum is labeled as YES/POSSIBLE/PASS (match); otherwise it is labeled NO/FAIL (no match). As an example, a normal spectrum should show YES/POSSIBLE/PASS when compared with a normal training set, and NO/FAIL with other training sets, and vice versa. Thus an unambiguous and objective discrimination can be achieved, as spectra are matched against all training sets before making a decision. All malignant spectra show "match," and all normal spectra show "no match" against a malignant training set (Table 2). In this table spectra 1–34 are malignant tissue spectra, and spectra 35–72 were recorded from normal tissues. Thus the sensitivity and specificity obtained by the true-positive and true-negative approach is 100%, as indicated in Table 1. However, as mentioned previously, sensitivity and specificity calculations based on a smaller number of subjects could be erroneous.

Thus, the results of the pilot study suggest that Raman spectroscopy can be used for discriminating normal and malignant ovarian tissues. Furthermore, the data analysis using the limit test approach is valuable from the clinical point of view, because once training sets are developed for different pathological conditions, a clinician or technician can directly match a recorded spectrum, and decision can be made more objectively, unambiguously, and rapidly.

CONCLUSIONS

Management of ovarian cancers poses a serious challenge, due to both a lack of reliable screening methods for detection and diagnosis at early stages, and lack of adequate treatment modalities for late stages. Intraoperative laparoscopy/laparotomy followed by histopathology/frozen section pathology can often determine the outcome. The present study was aimed at exploring an alternative modality of discriminating normal from malignant ovarian tissues by using conventional Raman spectroscopy. Spectral signatures of malignant tissues can be differentiated by the presence of additional biomolecules such as proteins, lipids, and DNA, from spectra of normal tissues. Discriminating algorithms, score of factor, Mahalanobis distance, spectral residuals, and limit test are employed in the analysis, and provide good classification of normal and malignant tissues. Among these methods, the limit test approach not only yielded the most accurate classification (100% specificity and sensitivity), but also provided unambiguous and objective discrimination. Furthermore, this approach is easily adaptable to routine clinical conditions and facilitates diagnosis of ovarian cancers by minimally-skilled personnel. Prospectively by developing models for other ovarian pathological conditions and rigorous evaluation of the models, these methods can be adapted to use as an intraoperative procedure for accurate diagnosis and detection of surgical margins during laparotomy using a suitable fiberoptic probe.

REFERENCES

1. Colombo, N., Van Gorp, T., Parma, G., et al. (2006). Ovarian cancer. Crit. Rev. Oncol. Hematol. 60, 159–179.
2. Parkin, D.M., Bray, F., Ferlay, J., and Pisani, P. (2005). Global cancer statistics, 2002. CA Cancer J. Clin. 55, 74–108.
3. Brewer, A.M., Johnson, K., Follen, M., Gershenson, D., and Bast, R. Jr. (2003). Prevention of ovarian cancer: Intraepithelial neoplasia. Clin. Cancer Res. 9, 20–30.
4. Ilvan, S., Ramazanoglu, R., Akyildiz, U.E., Calay, Z., Bese, T., and Oruc, N. (2005). The accuracy of frozen section (intraoperative consultation) in the diagnosis of ovarian masses. Gynecol. Oncol. 97, 395–399.
5. Boriboonhirunsarn, D., and Sermboon, A. (2004). Accuracy of frozen section in the diagnosis of malignant ovarian tumor. J. Obstet. Gynaecol. Res. 30, 349–399.
6. Hanlon, E.B., Manoharan, R., Koo, T.-W., et al. (2000). Prospects for *in vivo* Raman spectroscopy. Phys. Med. Biol. 45, R1–R59.
7. Diem, M., Romeo, M., Boydston-White, S., Miljkovic, M., and Matthaus, C. (2004). A decade of vibrational micro-spectroscopy of human cells and tissue. Analyst. 129, 880–885.
8. Wagnieres, G.A., Star, W.M., and Wilson, B.C. (1998). *In vivo* fluorescence spectroscopy and imaging for oncological applications. Photochem. Photobiol. 68, 603–632.
9. Kartha, V.B., Kurien, J., Rai, L., Mahato, K.K., Krishna, C.M., Santhosh, C. (2005). *Diagnosis at the Molecular Level: Analytical Laser Spectroscopy for Clinical Applications in Photoelectrochemistry and Photobiology in Environment, Energy and Fuel*. (Kaneko, S, Viswanathan, B, Funasaka, K, eds.), Trivandrum, India: Research Signpost, pp. 153–221.
10. Brewer, M., Utzinger, U., Silva, E., et al. (2001). Fluorescence spectroscopy for *in vivo* characterisation of ovarian tissue. Laser Surg. Med. 29, 128–135.
11. Utzinger, U., Brewer, A.M., Silva, E., et al. (2001). Reflectance spectroscopy for *in vivo* characterization of ovarian tissue. Lasers Surg. Med. 28, 56–66.
12. Donald, C.M., Nayak, L.P., Schaefer, S., Yingzhong, S., and Vinson, M. (1998). A unified theory of carcinogenesis based on order-disorder transitions in DNA structure as studied in the human ovary and breast. Proc. Natl. Acad. Sci. 95, 7637–7642.
13. Lieber, A.C., Molpus, K., Brader, K., and Mahadevan Jansen, A. (2000). Diagnostic tool for early detection of ovarian cancers using Raman spectroscopy. Proc. SPIE. 3918, 129–134.

14. Petricoin, E.F., Ardekani, A.M., Hitt, B.A., et al. (2002). Use of proteomic patterns in serum to identify ovarian cancer. Lancet. 359, 572–577.
15. Murali Krishna, C., Sockalingum, G.D., Rani Bhat, A., et al. (2007). FTIR and Raman microspectroscopy of normal, benign and malignant formalin-fixed ovarian tissues. Anal. Bioanal. Chem. 387, 1649–1656.
16. Murali Krishna, C., Sockalingum, G.D., Venteo, L., et al. (2005). Evaluation of the suitability of *ex vivo* handled ovarian tissues for optical diagnosis by Raman microspectroscopy. Biopolymers. 79, 269–276.
17. Malini, R., Venkatakrishna, K., and Kurien, J. (2006). Discrimination of normal, inflammatory, premalignant and malignant oral tissue: A Raman spectroscopy study. Biopolymers. 81, 179–193.
18. Murali Krishna, C., Prathima, N.B., Malini, R., et al. (2006). Raman spectroscopy studies for diagnosis of cancers in human uterine cervix. Vib. Spectrosc. 4, 136–141.
19. Chowdary, M.V.P., Kumar, K.K., Kurien, J., Mathew, S., and Murali Krishna, C. (2006). Discrimination of normal, benign, and malignant breast tissues by Raman spectroscopy. Biopolymers. 83, 556–569.
20. Kalyan, K.K., Anand, A., Chowdary, M.V.P., et al. (2007). Discrimination of normal and malignant stomach mucosal tissues by Raman spectroscopy: A pilot study. Vib. Spectrosc. 44, 382–387.
21. Chowdary, M.V.P., Kumar, K.K., Thakur, K., et al. (2007). Discrimination of normal and malignant mucosal tissue of colon by Raman spectroscopy, Photomed. Laser Surg. 25, 269–274.
22. Parker, E.S. (1983). Applications of infrared and Raman and resonance, in: *Raman Spectroscopy in Biochemistry*. New York: Plenum Press.
23. Tonge, P.J., and Carey, P.R. (1993). *Biomolecular Spectroscopy Part A, Advances in Spectroscopy*. R.J.H. Clark and R.E. Hester (eds.). Chichester, UK: John Wiley and Sons, Vol. 20, Chap. 3, pp. 129–133.
24. PLS Plus/IQ, Galactic Industries Corporation, 1991–1999.
25. Mahalanobis, P.C. (1936). On the generalized distance in statistics. Proc. Natl. Inst. Sci. India. 2, 249–255.

Address reprint requests to:
Dr. C. Murali Krishna, Ph.D.
Scientific Officer "E" and Principal Investigator
Chilakapati Laboratory
ACTREC, TMC
Khargar, Sector "22"
Navi Mumbai, 410208, India

E-mail: mchilakapati@actrec.gov.in
pittu1043@gmail.com
krishna.murali@uni-reims.fr